

1 **Benefit Transfer Loops Turn Cheating into a Scaffold for Microbial Diversity**

2 Jiqi Shao<sup>1,2</sup>, Yinxian Li<sup>3,4</sup>, Shaohua Gu<sup>1,2</sup>, Xiaoyi Zhang<sup>1</sup>, Shaopeng Wang<sup>5</sup>, Xueming  
3 Liu<sup>6</sup>, Zhiyuan Li<sup>1,7\*</sup>

4

5 <sup>1</sup> Center for Quantitative Biology, Academy for Advanced Interdisciplinary Studies,  
6 Peking University, Beijing 100871, China.

7 <sup>2</sup> Current Affiliation: College of Resources and Environmental Sciences, State Key  
8 Laboratory of Nutrient Use and Management (SKL-NUM), National Academy of  
9 Agriculture Green Development, China Agricultural University, Beijing 100193, China.

10 <sup>3</sup> School of Physics, Peking University, Beijing, 100871, China.

11 <sup>4</sup> Current Affiliation: Department of Physics, University of Illinois, 1110 W. Green Street,  
12 Urbana, Illinois 61801, United States.

13 <sup>5</sup> Institute of Ecology, College of Urban and Environmental Science and State Key  
14 Laboratory for Vegetation Structure, Function and Construction(VegLab), Peking  
15 University, Beijing, China.

16 <sup>6</sup> School of Artificial Intelligence and Automation, State Key Laboratory of Digital  
17 Manufacturing Equipment and Technology, Institute of Medical Equipment Science and  
18 Engineering, Huazhong University of Science and Technology, Wuhan, China.

19 <sup>7</sup> Peking-Tsinghua Center for Life Sciences, Academy for Advanced Interdisciplinary  
20 Studies, Peking University, Beijing 100871, China.

21

22 \*Correspondence: [zhiyuanli@pku.edu.cn](mailto:zhiyuanli@pku.edu.cn)

23

24

25 **Keywords:** Tragedy of the commons, Siderophores, Niche construction, Network  
26 percolation, Microbial coexistence

27

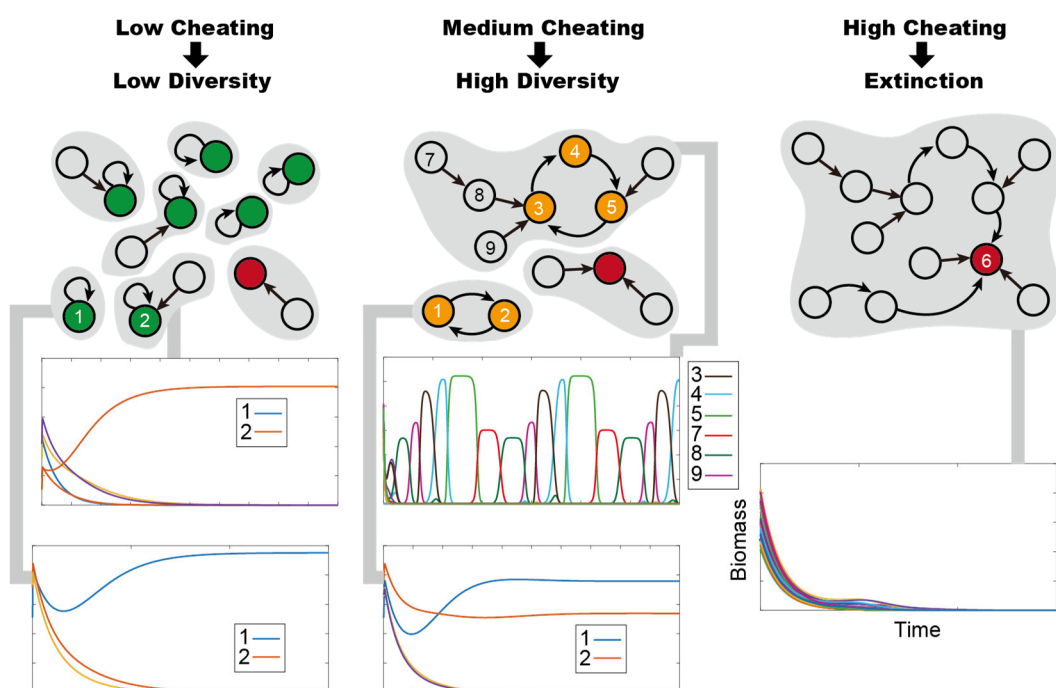
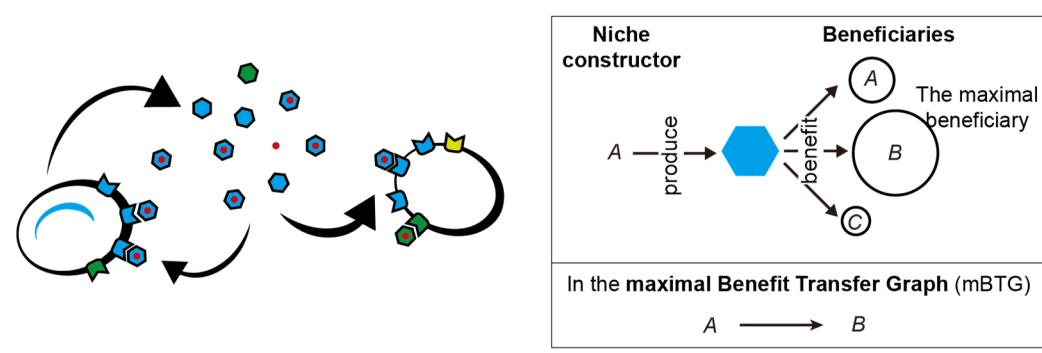
28 **Abstract**

29 Niche construction drives ecological dynamics, yet the tragedy of the commons predicts  
30 that non-contributing cheaters will undermine cooperation. Here, we studied microbial iron  
31 competition by combining dynamic modeling with benefit flow graphs, demonstrating that  
32 moderate cheating is not merely tolerated but essential for diversity. In small communities,  
33 mutual exploitation forms closed loops enabling steady or dynamic coexistence. In larger  
34 communities, we uncovered a paradox: increasing cheating breadth promotes community-  
35 level extinction, yet fosters higher biodiversity in surviving communities. We resolve this  
36 paradox by mapping ecological dynamics onto the topology of the “Maximal Benefit  
37 Transfer Graph”, which predicts community fate through its core structure. Broad cheating  
38 eliminates the self-loop core that drives competitive exclusion, but increases “terminator”  
39 sinks that cause collapse. However, when communities avoid these sinks, cheating  
40 aggregates the network and generates cyclic loops to enable coexistence. Thus, structured  
41 exploitation acts not as destabilizing vulnerability but as necessary architecture for  
42 biodiversity.

43

44

45 **Graphical Abstract**



46

47 How does 'cheating' affect microbial biodiversity? By mapping the strongest benefit flows  
48 between species, we discovered a topological rule for survival. While too much cheating  
49 creates dead-ends that crash the system, moderate cheating connects species into self-  
50 sustaining loops. These "exploitation cycles" act as a scaffold, supporting high diversity  
51 and complex population.

52

53

54

55 **Introduction**

56 Niche construction drives ecological dynamics[1], yet the “tragedy of the commons”  
57 predicts that non-contributing cheaters should undermine cooperative systems[2].  
58 Microbial siderophores represent a classic model of this dilemma: microbes secrete costly  
59 iron-scavenging molecules as public goods, which are then up taken via specific membrane  
60 receptors[3]. While functionally straightforward, siderophore systems display remarkable  
61 complexity stemming from two key features[4]: (1) extraordinary chemical diversity  
62 comprising at least a thousand structures[5]; and (2) high receptor specificity, creating  
63 “lock-and-key” patterns where receptors bind only specific siderophore subsets[6]. This  
64 specificity generates a rich ecological landscape where microbes possessing matching  
65 receptors can exploit “foreign” siderophores[7], forging intricate networks of competition,  
66 cooperation, and cheating[8].

67

68 This complexity makes siderophore-mediated interactions an ideal system for addressing  
69 a central puzzle in ecological theory: how does biodiversity persist in the face of cheating[9-  
70 11]? Classical theory suggests cheaters should outcompete producers, yet producers and  
71 cheaters coexist broadly in nature [12]. Observations in the *Pseudomonas* genus further  
72 complicate this picture: while pathogenic strains often exhibit extreme strategies with  
73 isolated iron-interaction networks, more diverse environmental isolates likely to adopt  
74 “partial-producers” strategies that producing siderophores while cheating on others[6]. A  
75 fundamental challenge lies in bridging scales: how do fine-grained molecular attributes,  
76 including structural diversity and receptor specificity, give rise to macro-scale ecological  
77 patterns? While previous studies have explored siderophore dynamics in biofilms or  
78 pairwise competitions[13, 14], they often overlook the emergent properties of networks  
79 formed by multiple siderophore types [15-17]. Understanding how biodiversity persists in  
80 complex communities requires bridging the gap between molecular-level interaction  
81 networks and emergent ecosystem dynamics[18].

82

83 Here, we develop a general theoretical framework that integrates consumer-resource  
84 dynamics with graph-theoretic representation of benefit flows, to systematically address  
85 these questions. Through simulations and analytical derivations, we prove that cheating is  
86 actually required for stable and oscillatory coexistence in small communities. In large  
87 communities, we uncover a paradox: increasing the breadth of cheating heightens the risk  
88 of community-level extinction, yet fosters higher biodiversity within surviving communities.  
89 By mapping ecological dynamics onto a “maximal Benefit Transfer Graph,” we identify the  
90 graph’s core structure as a powerful predictor of ecological outcomes, explaining cheating’s  
91 paradoxical role: Increased cheating pervasiveness connects species through network  
92 percolation, simultaneously expanding the “terminator” core driving extinction and the  
93 cyclic core enabling coexistence. Thus, our findings reveal a universal topological rule:  
94 structured exploitation acts not as a destabilizing vulnerability but as a necessary  
95 architecture for diversity. This principle extends beyond iron competition to broadly explain  
96 persistence in systems governed by directed benefit transfers, from extracellular enzyme  
97 hydrolysis to complex metabolic cross-feeding networks.

98 **Results**

99 **A Generalized Framework for Siderophore-mediated Interactions**

100 To link molecular specificity with ecological dynamics, we developed an integrated  
101 framework coupling dynamic modeling with network topology (Fig. 1, SI Appendix, Section  
102 1). Our dynamic model extends classical chemostat equations by incorporating diverse  
103 siderophore-receptor pairs, where growth depends on both iron uptake and primary  
104 metabolism (Fig. 1A). The model incorporates two key biological constraints: (1) a  
105 metabolic trade-off (parameter  $\alpha$ ), where species  $i$  allocate limited resources between  
106 growth ( $\alpha_{i0}$ ) and siderophore production ( $\alpha_{ij}$  for siderophore type  $j$ , under the constrain  
107  $\alpha_{i0} + \sum_{j=1}^{N_{\text{sid}}} \alpha_{ij} = 1$ ); and (2) a receptor profile (parameter  $\nu$ ), which dictates the specificity  
108 of iron uptake ( $\nu_{ij}$  represents the fraction of receptors dedicated to siderophore type  $j$  in  
109 species  $i$ , under the constrain  $\sum_{j=1}^{N_{\text{sid}}} \nu_{ij} = 1$ ).

110 The dynamic model tracks three sets of variables: (1) Microbial biomass concentration  $M_i$   
111 for each species  $i = 1, 2, \dots, N_{\text{spe}}$ ; (2) concentrations of each siderophore type  $R_j$  ( $j =$   
112  $1, 2, \dots, N_{\text{sid}}$ ); (3) Free iron concentration  $R_{\text{iron}}$ :

$$\frac{dM_i}{dt} = M_i \cdot \left( \gamma \cdot \alpha_{i0} \cdot \sum_j \nu_{ij} \cdot J_j - d \right) + \sigma, \quad (1)$$

where  $i = 1, \dots, N_{\text{spe}}$ .

113

$$\frac{dR_j}{dt} = \sum_i M_i \cdot \alpha_{ij} \cdot \epsilon_j - d \cdot R_j, \quad \text{where } j = 1, \dots, N_{\text{sid}}. \quad (2)$$

114

$$\frac{dR_{\text{iron}}}{dt} = d \cdot (R_{\text{supply}} - R_{\text{iron}}) - \sum_{i,j} M_i \cdot \nu_{ij} \cdot J_j. \quad (3)$$

115

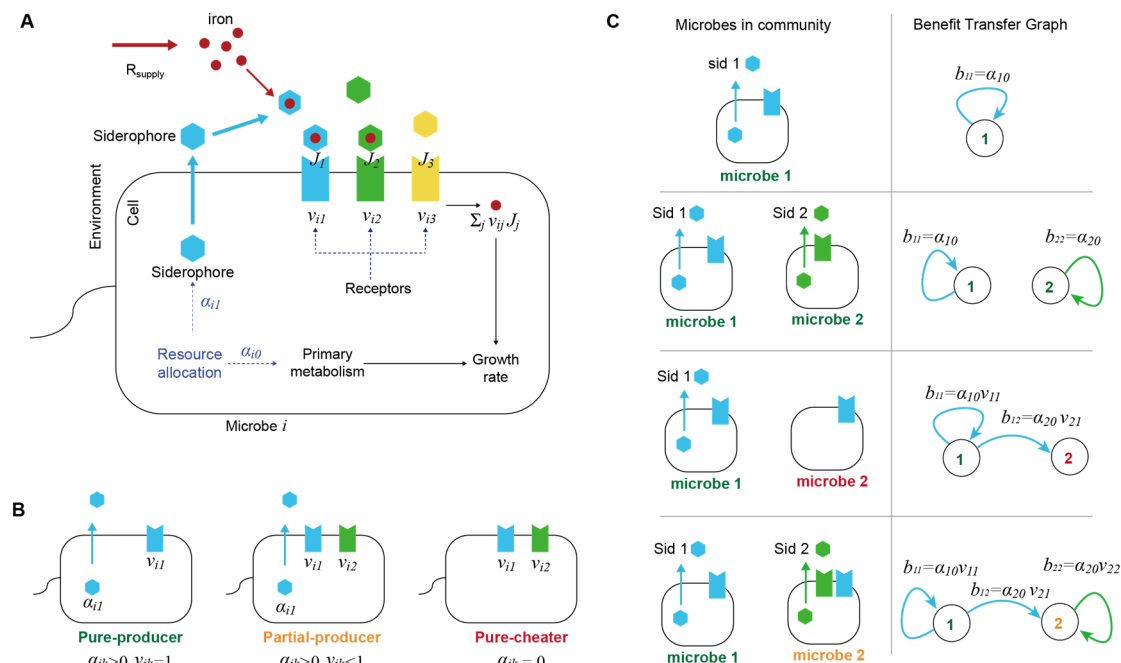
116 Varying parameters  $\alpha$  and  $\nu$  generates a continuum of strategies, from "pure-producers"  
117 (exclusively utilizing their own siderophores) to "pure-cheaters" (no production) and "partial  
118 producers" (producing one siderophore while exploiting several other types) (Fig. 1B).

119

120 Crucially, we mapped these biochemical interactions onto a "Benefit Transfer Graph" (BTG)  
121 to quantify ecological dependencies (Fig. 1C). In this directed graph, nodes represent  
122 species, and edges represent the flow of growth benefits from a siderophore producer to  
123 its beneficiaries. An edge exists if a species possesses receptors matching another's  
124 siderophore, with the weight  $b_{m1,m2}$  quantifying the specific growth gain species  
125  $m2$  derives from species  $m1$ 's production:

$$b_{m1,m2} = \begin{cases} 0, & \text{if } \alpha_{m1,j} = 0 \text{ for all } j \\ \alpha_{m2,0} \cdot \nu_{m2,j}, & \text{if } \alpha_{m1,j} > 0 \end{cases} \quad (4)$$

126 This abstraction allows us to translate complex kinetic systems into topological structures,  
 127 analyzing how benefit transfers drive community assembly.



128

129 **Figure 1. Framework for modeling siderophore-mediated interaction and benefit**  
 130 **transfer in microbial communities.**

131 (A) Overview of the siderophore-mediated iron uptake. Microbes allocate internal  
 132 resources between growth ( $\alpha_{i0}$ ) and the production of siderophores ( $\alpha_{ij}$  for  $j > 0$ ).  
 133 Secreted siderophores form siderophore-iron complexes, which are taken up via type-  
 134 specific receptors with allocation fractions  $v_{ij}$ . Different types of siderophores with their  
 135 matching receptors are distinguished by colors.

136 (B) Microbial iron-scavenging strategies. Microbes are categorized into three major classes  
 137 by siderophore production and uptake patterns: (i) “Pure-producers,” which produce and  
 138 exclusively utilize their own siderophores; (ii) “Partial-producers,” which produce/utilize  
 139 their own siderophores and also exploit foreign siderophores; (iii) “Pure-cheaters,” which  
 140 rely entirely on siderophores produced by others.

141 (C) Benefit Transfer Graph (BTG). Left panels illustrate example siderophore-mediated interactions;  
 142 right panels show their BTG representations: Nodes denote species, and  
 143 directed edges represent benefit transfer from siderophore producers to beneficiaries.  
 144 Edge colors correspond to siderophore types.

145

## 146 **Closed Benefit Loops Drive Transitions from Exclusion to Coexistence and Chaos**

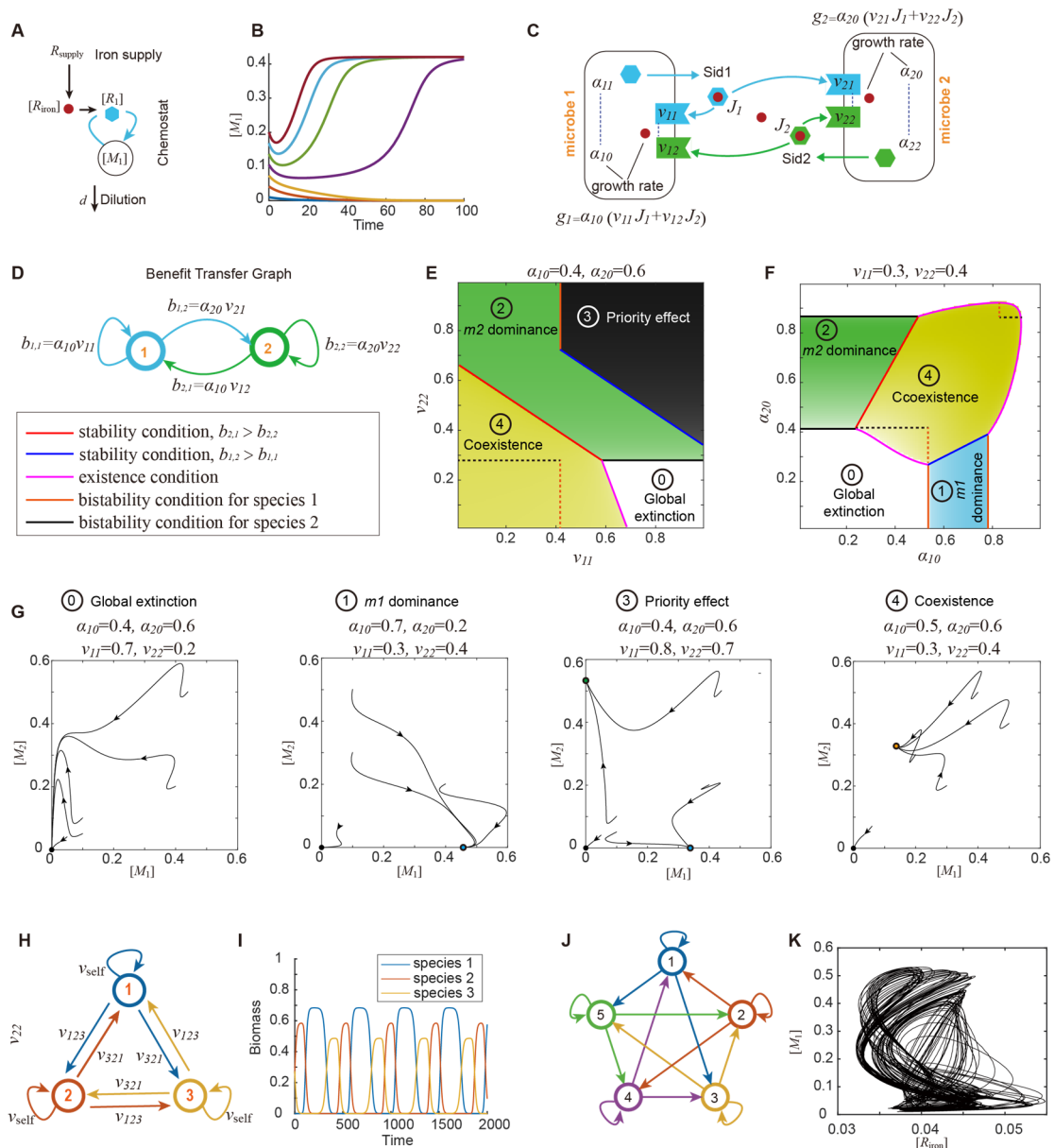
147 We first analyzed minimal community motifs to dissect the topological rules of coexistence.  
 148 In single-species systems with only one producer (Fig. 2A), the Benefit Transfer Graph  
 149 only consists of self-loops. Dynamic modeling reveals that siderophore-mediated positive

150 feedback creates an Allee effect [19], leading to bistability where survival depends on initial  
151 biomass thresholds (Fig. 2B; SI Appendix, Section 2). Consequently, when two pure-  
152 producers compete, they are driven to competitive exclusion: either one species becomes  
153 completely dominant, or the system exhibits priority effects in which the final winner is  
154 determined by who is initially more abundant (SI Appendix, Section 3)

155 Stable coexistence emerges only when species adopt “partial-producer” strategies,  
156 forming a closed mutual cheating loop in the BTG (Fig. 2C–D). Analytically, we derived that  
157 each species must deliver greater growth benefits to its competitor than to itself ( $b_{2,1} >$   
158  $b_{2,2}$ ,  $b_{1,2} > b_{1,1}$ , SI Appendix, Section 4). Strikingly, this mutual exploitation generates a  
159 synergistic rescue effect: in parameter regimes where single species would collapse, the  
160 combined siderophore pool allows the mutualistic pair to survive (Fig. 2E–G).

161 Expanding these loops to multi-species motifs identifies key topologies that enable  
162 dynamic coexistence. In three-species systems, an intransitive “rock–paper–scissors” BTG  
163 loop (Fig. 2H) generates sustained population oscillations (Fig. 2I). Bifurcation analysis  
164 demonstrates that increasing self-reliance drives a transition from oscillatory coexistence  
165 to competitive exclusion via Heteroclinic bifurcation[20], while balanced benefit flows favor  
166 stable coexistence over limit cycles (SI Appendix, Section 5).

167 As the interaction network grows more complex, such as in five-species motifs with  
168 overlapping loops (Fig. 2J), coupled feedback can drive the system into deterministic chaos  
169 (Fig. 2K). Similarly, increasing self-reliance progressively drives transition from chaotic  
170 dynamics to stable periodic cycles and, eventually, to exclusion. Collectively, these results  
171 demonstrate that closed benefit-transfer loops serve as the structural scaffold for diversity:  
172 short mutual loops support stable coexistence, while longer cycles enable dynamic  
173 fluctuations.



174

175 **Figure 2. Rules governing siderophore-mediated iron interactions in single- and two-  
176 species models.**

177 A. Schematic of the single-species chemostat model with iron supply  $R_{\text{supply}}$  and  
178 dilution rate  $d$ . Variables  $[R_{\text{iron}}]$ ,  $[M_1]$ ,  $[R_1]$  denote the concentration of free iron,  
179 microbial biomass, and siderophore, respectively.

180 B. Time courses of biomass ( $M_1$ ) starting from different initial inoculations, illustrating the  
181 threshold-dependent survival.

182 C. Schematic of a two-species system where two pure-producers compete. Each  
183 species secretes and exclusively utilizes its own siderophore type (blue for species 1,  
184 green for species 2).

185 D. The Benefit Transfer Graph (BTG) corresponding to (C). Nodes represent species;  
186 edges represent the benefit flow. This graph features self-loops ( $b_{1,1}$ ,  $b_{2,2}$ ) and cross-  
187 species benefit transfers ( $b_{1,2}$ ,  $b_{2,1}$ )

188 E-F. Phase diagram spanning the receptor profile ( $v_{11}$ - $v_{22}$  for E) and growth allocation  
189 ( $\alpha_{10}$  –  $\alpha_{20}$  for F). Distinct ecological outcomes are color-coded and numbered. Color  
190 intensity is proportional to the total steady-state biomass.

191 G. Representative state-space simulation dynamics projected onto the  $M_1$ - $M_2$  plane,  
192 parameters are from four different regimes in (E)-(F). Arrows denote the directionality  
193 of trajectories. Solid circles indicate stable fixed points.

194 H. BTG of a three-species system. Blue, orange, and yellow arrows represent benefit  
195 transfers mediated by different siderophores produced by species 1, 2, and 3,  
196 respectively. Two rock-paper-scissors loops emerge: clockwise (characterized by  $v_{321}$ )  
197 and counterclockwise (characterized by  $v_{123}$ ). Self-loops indicate self-utilization ( $v_{\text{self}}$ )

198 I. Representative time courses showing sustained oscillations in the system of (H).

199 J. BTG of a five-species system.

200 K. State-space projection onto the  $R_{\text{iron}}$ - $M_1$  plane showing a chaotic trajectory.

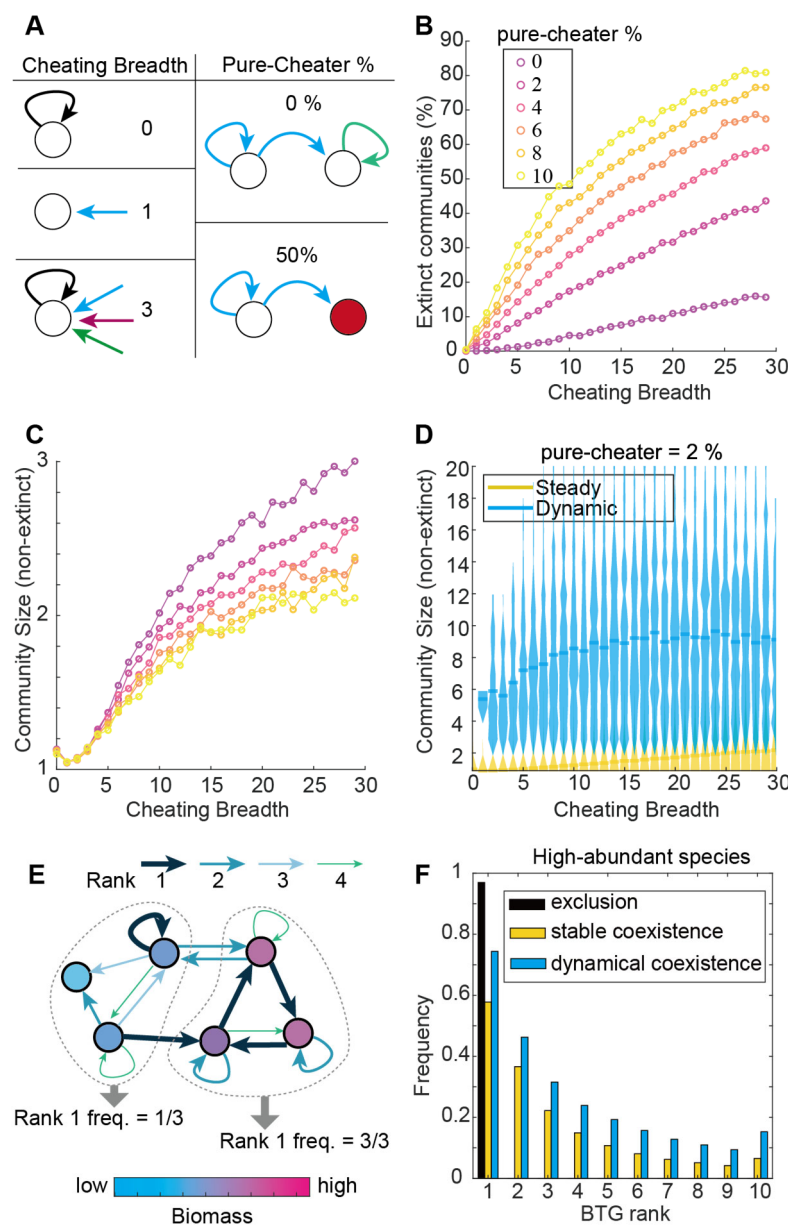
201

202 **The Paradox of Cheating in Large Communities**

203 We extended our framework to complex ecosystems by simulating  $1.5 \cdot 10^6$  communities  
204 ( $N_{\text{spe}} = 50$ ) with varying “cheating breadth” (the average number of foreign siderophores a  
205 species can exploit) and fractions of “pure-cheaters” (Fig. 3A). Simulation outcomes reveal  
206 an unintuitive paradox. On one hand, broad cheating and high pure-cheater ratio act as  
207 destabilizing forces, monotonically increasing the probability of community-wide extinction  
208 (Fig. 3B).

209 On the other hand, within non-extinct communities (having at least one surviving species),  
210 cheating promotes biodiversity. Species richness increases monotonically with cheating  
211 breadth (Fig. 3C), and these diverse communities are more likely to exhibit dynamic  
212 behaviors (oscillations or chaos) (SI Appendix, Section 6). Notably, dynamic communities  
213 consistently support larger populations than stable ones, suggesting that temporal  
214 fluctuations create niches for species maintenance (Fig. 3D).

215  
216 The paradox of cheating breadth implies that surviving communities must harbor non-  
217 random interaction structures that enable persistence. To identify these structures, we  
218 analyzed the Benefit Transfer Graph within each non-extinct community. For every  
219 siderophore producer  $i$ , we ranked all its outgoing benefit edges ( $b_{ij}$ ) by magnitude,  
220 designating the single strongest flow as the “Rank-1 edge” (Fig. 3E). Notably, we found  
221 that the subgraph formed by surviving species is overwhelmingly dominated by these  
222 Rank-1 incoming edges (Fig. 3F), far exceeding their frequency in randomly assembled  
223 subgraphs (SI Appendix, Section 6). This finding suggests that community fate is not  
224 determined by average interaction strengths, but by a specific topological backbone formed  
225 by maximal benefit flows.



227

228

229 **Figure 3. Cheating breadth elevates both extinction risk and community diversity**

230

231 A. Definitions of cheating breadth (number of exploitable foreign siderophore types) and  
232 pure-cheater ratio.

233 B. Probability of community-level extinction increases with both cheating breadth and  
234 pure-cheater ratio (ratio is color-coded; consistent across panels B–C).

235 C. In non-extinct communities, species richness increases with cheating breadth but  
236 decreases with pure-cheater ratio.

237 D. Violin plots showing non-extinct community size distributions for steady (yellow) versus  
238 dynamic (green) outcomes (pure-cheater ratio = 2%), under different cheating breadth.  
239 Dynamic communities consistently support higher biodiversity.

240 E. Schematic illustrating edge ranking in BTGs, where edges from producers  $i$  are ranked  
241 by their weights  $b_{ij}$ . Two subgraphs formed by low-biomass species (left) and high-

242 biomass species (right) are bracketed by dashed lines, with the relative frequency of  
243 Rank-1 incoming edges shown below.

244 F. Rank frequency distribution of benefit transfer edges in BTGs. Top-ranked edges were  
245 enriched in subgraphs formed by high-abundance species (biomass  $> 10^{-3}$ )

246 **The Maximal Benefit Transfer Graph Resolves the Cheating Paradox**

247 To decode the structural basis of the cheating paradox, we formalized the "Rank-1"  
248 backbone as a maximal Benefit Transfer Graph (mBTG). By retaining only the strongest  
249 outgoing benefit edge for each producer, the mBTG assumes the topology of a directed  
250 pseudoforest, a graph class where every node has at most one outgoing edge (Fig. 4A).  
251 A central feature of such graphs is their decomposition into Weakly Connected  
252 Components (WCCs), which are groups of nodes connected by paths regardless of  
253 direction. In directed pseudoforests, benefit flows within each WCC inevitably converge  
254 to a unique "Core": the minimal subset of nodes with no outgoing edges to the rest of the  
255 graph (Fig. 4B).

256 We discovered that the topology of this Core serves as a potent predictor of community  
257 fate, achieving around 80% classification accuracy. Irrespective of initial conditions,  
258 asymptotic biomass consistently concentrates within a single WCC, and specifically  
259 within its core (SI Appendix, Section 7). This indicates that each WCC represents a  
260 distinct basin of attraction, with the core acting as the structural and dynamic nucleus.  
261 Characterizing these cores by their "loop length" (the number of edges forming the core)  
262 reveals three distinct architectures that dictate ecological outcomes (Fig. 4B):

- 263 1. Sink Core (Loop length 0, W0 in Fig. 4B): A core consisting of a single pure-cheater  
264 acts as a resource "black hole," absorbing benefits without reciprocation. This  
265 topology leads to community extinction with 97% probability.
- 266 2. Self-loop Core (Loop length 1, W1 in Fig. 4B): A core formed by a producer benefiting  
267 maximally from itself leads to a steady state (Fig. 4C) where the core species  
268 survives alone, driving all others to exclusion (Fig. 4D).
- 269 3. Cyclic Core (Loop length  $\geq 2$ , W2 and W3 in Fig. 4B): A closed loop of two or more  
270 species supports coexistence. Notably, as the loop length reaches three, the  
271 probability of entering oscillatory or chaotic attractors increases sharply (Fig. 4C).  
272 While species richness in steady-state systems plateaus at short loop lengths,  
273 dynamic systems continuously support higher diversity (Fig. 4D). These dynamic  
274 communities often harbor twice as many total survivors (biomass  $> 10^{-6}$ ) as high-  
275 abundance species (biomass  $> 10^{-3}$ ), suggesting that oscillatory dynamics enable  
276 rare species to persist by intermittently accessing benefits from abundant ones (Fig.  
277 4D).

278 This topological framework resolves the paradox of cheating breadth. The mBTG is  
279 composed of four functional node types, whose abundance changes by cheating breadth  
280 (Fig. 4E, SI Appendix, Section 8):

281 1. “Self-loop” Maximal Beneficiaries (MBs): Producers that gain the highest benefit from  
282 their own siderophores. These form Self-loop Cores, driving exclusion. However,  
283 increasing cheating breadth expands the pool of potential recipients, “diluting” a  
284 producer’s probability of retaining its own siderophore as the maximal benefit (Fig. 4F).  
285 This causes a monotonic decline in exclusion-driving Self-loops.

286 2. “Connector” MBs: Partial-producers possessing both incoming edges and an outgoing  
287 edge. This type benefits most from foreign siderophores while producing a siderophore  
288 whose maximal beneficiary is not itself. They are the essential “glue” for Cyclic Cores,  
289 linking species into loops that support stable or dynamic coexistence.

290 3. “Terminator” MBs: Nodes with incoming edges but no outgoing edges, corresponding  
291 exclusively to pure-cheaters. They form Sink Cores. Selection of maximal beneficiaries  
292 probabilistically favors species with higher growth allocation (like pure-cheaters with  
293  $\alpha_0 = 1$ ), and broader cheating amplifies this bias (Fig. 4G), causing a surge in  
294 Terminator MBs.

295 4. “Leaf” Nodes: Species with no incoming edges. The number of Leaf nodes increases  
296 as cheating breadth expands, indicating that incoming edges concentrate  
297 disproportionately on a small subset of species. This trend can also be explained by  
298 the increased bias towards high- $\alpha_0$  species, which leads to a heavy-tailed in-degree  
299 distribution in which a small set of “super-beneficiaries” capture maximal benefits from  
300 many sources whereas most species get none.

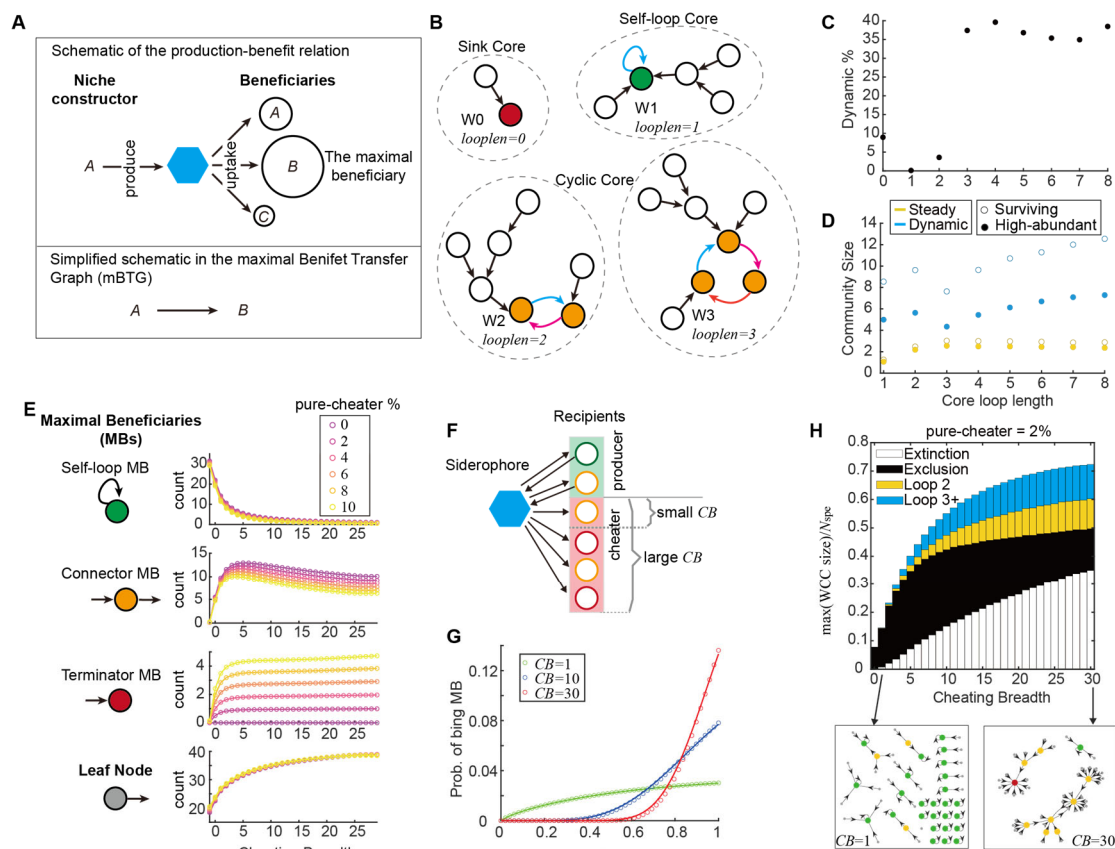
301

302 Taken together, as cheating breadth increases, the mBTG undergoes a percolation-like  
303 transition. The suppression of Self-loops releases outgoing edges, while the concentration  
304 of edges toward “super-beneficiaries” promotes the coalescence of fragmented  
305 components into a giant connected cluster (Fig. 4H). This reduces multi-stability, forcing  
306 the community into few dominant attractors. Thus, while broad cheating eliminates the self-  
307 loops that trigger exclusion, it forces the community to “gamble”: it either collapses into a  
308 Terminator Sink or stabilizes into a complex, high-diversity Cyclic Core. Cheating therefore  
309 does not always act as a destabilizing vulnerability, but can also provide the necessary  
310 architectural scaffold for biodiversity.

311

312

313



314

315 **Figure 4. Core loops of the maximal Benefit Transfer Graph (mBTG) predicts**  
 316 **community fate and resolves the cheating paradox**

317 A. Construction of the mBTG. For each producer, the single strongest outgoing benefit  
 318 flow defines the “maximal beneficiary,” forming a rank-1 directed edge.

319 B. Topology of the mBTG decomposes into Weakly Connected Components (WCCs),  
 320 each containing exactly one “Core” (colored nodes and edges). Four WCCs are  
 321 separated by dashed circles. Core classes (Sink, Self-loop, Cyclic) are marked on each  
 322 top.

323 C. Scatter plots showing the probability of entering dynamic attractors leaps at core loop  
 324 length of three.

325 D. Scatter plot showing how community size increases with core loop length, for steady-  
 326 state (yellow) and dynamic (blue) communities. Filled and open circles indicate high-  
 327 abundance and surviving species (biomass threshold  $10^{-3}$  and  $10^{-6}$ ), respectively.

328 E. Node classifications in mBTG (left) and how their counts change with cheating breadth  
 329 (right). Self-loop maximal beneficiaries (MBs) have edges directed to itself; Connector  
 330 MBs possess both incoming and outgoing edges; Terminator MBs have only incoming  
 331 edges and no outgoing edges; Leaf nodes have no incoming edges.

332 F. Probabilistic explanation that increasing cheating breadth expands the pool of potential  
 333 recipients, diluting the producer’s chance of retaining its own siderophore (Self-loop  
 334 MBs decline).

335 G. Broader cheating amplifies MB selection bias toward high- $\alpha_0$  species, creating heavy-  
 336 tailed in-degree distributions and promoting Terminator MBs (CB is abbreviation for  
 337 cheating breadth).

338 H. The percolation transition. The curve shows the fraction of nodes occupied by the  
339 largest WCC, which grows with cheating breadth. Colors under the curve indicate the  
340 proportion of WCCs governed by different core lengths. The system transitions from  
341 fragmented Self-loop Cores (exclusion) to giant components dominated by either  
342 Terminators (extinction) or Cyclic Cores (coexistence), with examples shown in bottom  
343 insets.

344

## 345 Discussion

346 In this study, we introduce an integrated framework that bridges molecular specificity,  
347 ecological dynamics, and network topology to resolve the "cheating paradox" in microbial  
348 communities. By mapping siderophore-mediated interaction dynamics to a maximal  
349 Benefit Transfer Graph (mBTG), we demonstrate that community fate, whether extinction,  
350 exclusion, or coexistence, is encoded in the core topology of benefit flows. Our findings  
351 challenge the classical view that cheating is purely detrimental. While unchecked cheating  
352 (Sink Cores) indeed drives collapse, structured exploitation (Cyclic Cores) acts as a  
353 necessary architectural scaffold for biodiversity.

354

355 The concept of niche construction traditionally emphasizes how organisms modify  
356 environments to their benefit, but it also creates vulnerabilities to exploitation[21]. While  
357 mechanisms such as spatial segregation[22], metabolic cross-feeding[23], and kin  
358 selection[24] have been proposed to resolve this dilemma, our model demonstrates that  
359 cheating itself can be transformed into an organizing force. This can be analogous to the  
360 central tenet of Modern Coexistence Theory, which posits that stable coexistence arise  
361 from either niche differentiation or fitness equivalence [25, 26]. Similarly, when microbes  
362 create multiple "chemical niches" by diverse siderophore types, partial-producers emerge  
363 as essential "loop connectors," linking distinct niches through their dual capacity to produce  
364 and exploit. This aligns with empirical observations in *Pseudomonas*, where partial-  
365 producers are associated with diverse, non-pathogenic communities, whereas pure  
366 strategies are linked to low diversity and pathogenicity[6].

367

368 This graph-theoretic framework bridges experiments, bioinformatics, and ecological  
369 theories. While kinetic parameters are often elusive in wild communities, the structure of  
370 the Benefit Transfer Graph can be inferred from genomic analysis[4] or cross-feeding  
371 assays[27]. By coarse-graining molecular specificity into topological motifs (WCCs and  
372 Cores), the mBTG approach can forecast community fate not only in systems governed by  
373 siderophore-mediated interactions, but also in other systems driven by shared chemical  
374 resources, such as extracellular enzyme hydrolysis[28], antibiotic degradation[29], or  
375 metabolic cross-feeding networks[30].

376

377 Percolation theory describes abrupt transitions from local connectivity to global connectivity  
378 [31]. Previously applied to physical connectivity like fragmented habitats [32, 33],  
379 percolation concepts now extend to abstract interaction networks [34]. Our Maximal Benefit

380 Transfer Graph (mBTG) exhibits distinctive percolation behavior shaped by its  
381 pseudoforest topology: increasing cheating breadth rapidly merges Weakly Connected  
382 Components into a giant component, while Strongly Connected Components (formed the  
383 cores) approach but never reach the percolation threshold. Under evolutionary dynamics,  
384 this structure self-organizes further. Pure-cheaters face extinction, driving the network  
385 toward self-sustaining structures composed by either Self-loops or Connector-based  
386 cycles. This mirrors autocatalytic set emergence, where mutually reinforcing cycles evolve  
387 spontaneously from random networks [35]. Biologically, this suggests that ecosystems  
388 operate near a critical point. Bacteria generally possess multiple siderophore receptors,  
389 ranging from 1–4 in *E. coli* to 20–30 in *Pseudomonas* and other environmental strains [7,  
390 36–38]. This range corresponds to the “near-critical spot” in our simulations—high enough  
391 to ensure global connectivity and diversity, yet structured enough to maintain stability.  
392

393 Our work provides a mechanistic foundation that grounds abstract ecological theory in  
394 molecular specificity. We show that siderophore-mediated interactions generate rich  
395 phenomena, ranging from synergistic rescue and priority effects to heteroclinic bifurcations.  
396 While phenomenological models highlight the role of intransitive interactions in maintaining  
397 diversity[39], our work identifies a concrete chemical basis for such dynamics. Furthermore,  
398 the emergence of oscillation and chaos supports theoretical predictions that non-  
399 equilibrium dynamics promote diversity through temporal niche partitioning[40].  
400

401 Our current framework relies on simplified assumptions to ensure analytical tractability,  
402 such as well-mixed environments and single-siderophore production. These simplifications  
403 point toward fruitful avenues for future exploration. For instance, incorporating spatial  
404 structure could reveal how biofilm stabilize or fragment large interaction loops [41], and  
405 integrating more interactions like nutrient competition and antibiotic antagonism would offer  
406 a more holistic ecological picture [42]. Additionally, incorporating evolutionary dynamics will  
407 be crucial to understand the selective origins of these topological motifs [8, 43]. Ultimately,  
408 these future complexities will build upon the fundamental principle established here:  
409 molecular specificity transforms the social dilemma of public goods, recasting cheating  
410 from a destabilizing threat into the structural scaffold of diverse ecosystems.  
411

## 412 **Acknowledgments**

413 This work is supported by National Natural Science Foundation of China (No. T2321001  
414 to ZL, 32588202 and 32425036 to SW, and T2422010 and 62172170 to XL), Fundamental  
415 and Interdisciplinary Disciplines Breakthrough Plan of the Ministry of Education of China  
416 (JYB2025XDXM502 to ZL), National Key Research and Development Programme of China  
417 (2022YFF0802103 to SW), the Peking-Tsinghua Center for Life Sciences, and the  
418 Fundamental Research Funds for Central Universities.

419 **Reference**

420 1. Laland, K.N., F.J. Odling-Smee, and M.W. Feldman, *Evolutionary consequences of*  
421 *niche construction and their implications for ecology*. Proceedings of the National  
422 Academy of Sciences, 1999. **96**(18): p. 10242-10247.

423 2. Jones, E.I., et al., *Cheaters must prosper: reconciling theoretical and empirical*  
424 *perspectives on cheating in mutualism*. Ecology letters, 2015. **18**(11): p. 1270-1284.

425 3. West, S.A., et al., *Social evolution theory for microorganisms*. Nat Rev Microbiol, 2006.  
426 **4**(8): p. 597-607.

427 4. Gu, S., et al., *Forging the iron-net: Towards a quantitative understanding of microbial*  
428 *communities via siderophore-mediated interactions*. Quantitative Biology, 2025. **13**(2):  
429 p. e84.

430 5. He, R.L., et al., *SIDERITE: Unveiling hidden siderophore diversity in the chemical*  
431 *space through digital exploration*. Imeta, 2024. **3**(2).

432 6. Gu, S., et al., *Siderophore synthetase-receptor gene coevolution reveals habitat- and*  
433 *pathogen-specific bacterial iron interaction networks*. Science Advances, 2025. **11**(3):  
434 p. eadq5038.

435 7. Gu, S., et al., *Feature sequence-based genome mining uncovers the hidden diversity*  
436 *of bacterial siderophore pathways*. eLife, 2024. **13**: p. RP96719.

437 8. Niehus, R., et al., *The evolution of siderophore production as a competitive trait*.  
438 Evolution, 2017. **71**(6): p. 1443-1455.

439 9. West, S.A., et al., *The social lives of microbes*. Annual Review of Ecology, Evolution,  
440 and Systematics, 2007. **38**: p. 53-77.

441 10. Smith, P. and M. Schuster, *Public goods and cheating in microbes*. Current Biology,  
442 2019. **29**(11): p. R442-R447.

443 11. Tarnita, C.E. and A. Traulsen, *Reconciling ecology and evolutionary game theory or*  
444 *"When not to think cooperation"*. Proc Natl Acad Sci U S A, 2025. **122**(14): p.  
445 e2413847122.

446 12. Sun, Z., et al., *Microbial cross-feeding promotes multiple stable states and species*  
447 *coexistence, but also susceptibility to cheaters*. Journal of Theoretical Biology, 2019.  
448 **465**: p. 63-77.

449 13. Eberl, H.J. and S. Collinson, *A modeling and simulation study of siderophore mediated*  
450 *antagonism in dual-species biofilms*. Theor Biol Med Model, 2009. **6**: p. 30.

451 14. Lerch, B.A., et al., *How public can public goods be? Environmental context shapes the*  
452 *evolutionary ecology of partially private goods*. PLoS Comput Biol, 2022. **18**(11): p.  
453 e1010666.

454 15. Shao, J., et al., *Siderophore-mediated iron partition promotes dynamical coexistence*  
455 *between cooperators and cheaters*. iScience, 2023. **26**(9): p. 107396.

456 16. Butaité, E., et al., *Siderophore cheating and cheating resistance shape competition for*  
457 *iron in soil and freshwater Pseudomonas communities*. Nat Commun, 2017. **8**(1): p.  
458 414.

459 17. O'Brien, S., C.T. Culbert, and T.G. Barraclough, *Community composition drives*  
460 *siderophore dynamics in multispecies bacterial communities*. BMC Ecology and  
461 Evolution, 2023. **23**(1): p. 45.

462 18. Leinweber, A., R. Fredrik Inglis, and R. Kümmerli, *Cheating fosters species co-*  
463 *existence in well-mixed bacterial communities*. The ISME Journal, 2017. **11**(5): p. 1179-  
464 1188.

465 19. Goswami, M., P. Bhattacharyya, and P.J.A.o.m. Tribedi, *Allee effect: the story behind*  
466 *the stabilization or extinction of microbial ecosystem*. 2017. **199**: p. 185-190.

467 20. Van Voorn, G.A., et al., *Heteroclinic orbits indicate overexploitation in predator-prey*  
468 *systems with a strong Allee effect*. Mathematical biosciences, 2007. **209**(2): p. 451-469.

469 21. Rankin, D.J., K. Bargum, and H. Kokko, *The tragedy of the commons in evolutionary*  
470 *biology*. Trends Ecol Evol, 2007. **22**(12): p. 643-51.

471 22. Waite, A.J., C. Cannistra, and W. Shou, *Defectors can create conditions that rescue*  
472 *cooperation*. PLoS computational biology, 2015. **11**(12): p. e1004645.

473 23. Morris, J.J., R.E. Lenski, and E.R. Zinser, *The Black Queen Hypothesis: Evolution of*  
474 *Dependencies through Adaptive Gene Loss*. mBio, 2012. **3**(2): p. 10.1128/mbio.00036-  
475 12.

476 24. Nowak, M.A., *Five rules for the evolution of cooperation*. Science, 2006. **314**(5805): p.  
477 1560-3.

478 25. Chesson, P., *Mechanisms of maintenance of species diversity*. Annual review of  
479 Ecology and Systematics, 2000. **31**(1): p. 343-366.

480 26. Levine, J.M., et al., *Beyond pairwise mechanisms of species coexistence in complex*  
481 *communities*. Nature, 2017. **546**(7656): p. 56-64.

482 27. Griffin, A.S., S.A. West, and A. Buckling, *Cooperation and competition in pathogenic*  
483 *bacteria*. Nature, 2004. **430**(7003): p. 1024-1027.

484 28. Gore, J., H. Youk, and A. van Oudenaarden, *Snowdrift game dynamics and facultative*  
485 *cheating in yeast*. Nature, 2009. **459**(7244): p. 253-256.

486 29. Yurtsev, E.A., et al., *Bacterial cheating drives the population dynamics of cooperative*  
487 *antibiotic resistance plasmids*. Mol Syst Biol, 2013. **9**: p. 683.

488 30. Goldford, J.E., et al., *Emergent simplicity in microbial community assembly*. Science,  
489 2018. **361**(6401): p. 469-474.

490 31. Saberi, A.A., *Recent advances in percolation theory and its applications*. Physics  
491 Reports, 2015. **578**: p. 1-32.

492 32. With, K.A., *Using Percolation Theory to Assess Landscape Connectivity and Effects of*  
493 *Habitat Fragmentation*, in *Applying Landscape Ecology in Biological Conservation*, K.J.  
494 Gutzwiller, Editor. 2002, Springer New York: New York, NY. p. 105-130.

495 33. Hunt, A.G. and M. Sahimi, *Flow, transport, and reaction in porous media: Percolation*  
496 *scaling, critical-path analysis, and effective medium approximation*. Reviews of  
497 Geophysics, 2017. **55**(4): p. 993-1078.

498 34. Clegg, T. and T. Gross, *Cross-feeding creates tipping points in microbiome diversity*.  
499 Proceedings of the National Academy of Sciences, 2025. **122**(19): p. e2425603122.

500 35. Jain, S. and S. Krishna, *Autocatalytic sets and the growth of complexity in an*  
501 *evolutionary model*. Physical Review Letters, 1998. **81**(25): p. 5684.

502 36. Watts, R.E., et al., *Contribution of siderophore systems to growth and urinary tract*  
503 *colonization of asymptomatic bacteriuria Escherichia coli*. Infection and immunity, 2012.  
504 **80**(1): p. 333-344.

505 37. Cornelis, P. and J. Bodilis, *A survey of TonB-dependent receptors in fluorescent*

506 38. *pseudomonads*. Environ Microbiol Rep, 2009. **1**(4): p. 256-62.

507 38. Yu, L., G. Xiong, and Z. Li, *Co-Evolutionary Characterization of PBP2 as the*  
508 *Predominant Siderophore Recognizer in Diverse Gram-Positive Bacteria*. bioRxiv,  
509 2025: p. 2025.09. 29.679136.

510 39. Allesina, S. and J.M. Levine, *A competitive network theory of species diversity*.  
511 Proceedings of the National Academy of Sciences, 2011. **108**(14): p. 5638-5642.

512 40. Hu, J., et al., *Emergent phases of ecological diversity and dynamics mapped in*  
513 *microcosms*. Science, 2022. **378**(6615): p. 85-89.

514 41. Momeni, B., A.J. Waite, and W. Shou, *Spatial self-organization favors heterotypic*  
515 *cooperation over cheating*. eLife, 2013. **2**: p. e00960.

516 42. Dubinkina, V., et al., *Multistability and regime shifts in microbial communities explained*  
517 *by competition for essential nutrients*. eLife, 2019. **8**: p. e49720.

518 43. Harrison, F., et al., *Optimised chronic infection models demonstrate that siderophore*  
519 *'cheating' in Pseudomonas aeruginosa is context specific*. The ISME journal, 2017.  
520 **11**(11): p. 2492-2509.

521